Translational Oncology 26 (2022) 101548

Contents lists available at ScienceDirect

Translational Oncology

journal homepage: www.elsevier.com/locate/tranon

Original Research

Nicaraven induces programmed cell death by distinct mechanisms according to the expression levels of Bcl-2 and poly (ADP-ribose) glycohydrolase in cancer cells

Lina Abdelghany [a,b], Tsuyoshi Kawabata [a,b], Shinji Goto [a,b], Keiichi Jingu [c], Tao-Sheng Li [a,b,*]

[a] Department of Stem Cell Biology, Atomic Bomb Disease Institute, Nagasaki University, 1-12-4 Sakamoto, Nagasaki 852-8523, Japan
[b] Department of Stem Cell Biology, Nagasaki University Graduate School of Biomedical Sciences, 1-12-4 Sakamoto, Nagasaki 852-8523, Japan
[c] Department of Radiation Oncology, Graduate School of Medicine, Tohoku University, Sendai, Japan

ARTICLE INFO

Keywords:
Nicaraven
PARG
Bcl-2
Parthanatos
Apoptosis
Cancer cells

ABSTRACT

The PARP-1 expression level and poly (ADP-ribosyl)ation activity in cancer markedly affect the therapeutic outcome. Nicaraven, a free radical scavenger has been found to inhibit PARP, but the effect on cancer cells is still unclear. In this study, we investigated the potential role and molecular mechanism of nicaraven on cancer cells. Using U937 lymphoma cells and HCT-8 colorectal cancer cells, we found that nicaraven moderately reduced the cell viability of both cells in a dose-dependent manner. Interestingly, nicaraven significantly induced apoptosis of U937 cells that are dominantly expressing Bcl-2 but induced PAR-dependent cell death (parthanatos) of HCT-8 cells that are highly expressing poly (ADP-ribose) glycohydrolase (PARG). Based on our data, nicaraven seems to induce programmed cell death through distinct mechanisms, according to the expression levels of Bcl-2 and PARG in cancer cells.

Introduction

Cancer cells commonly show upregulated expression of poly (ADP-ribose) polymerases (PARPs) [1,2]. PARPs mediate poly (ADP-ribosyl) ation (PARylation), which plays an important role in DNA repair [3]. PARP-1 catalyzes PARylation, one of the post-translational modifications of proteins, using NAD as a substrate [4,5]. The PARylation activity of PARP-1 is activated by DNA breaks [6]. Suppressing PARylation activity by PARP-1 inhibitors has been clinically applied for the treatment of various types of cancers [7–9]. PAR is catabolized mainly by poly (ADP-ribose) glycohydrolase (PARG) in a process called dePARylation [10]. Thus, targeting dePARylating enzymes such as PARG, has attracted considerable interest in cancer therapy [11].

Nicaraven was originally developed as a hydroxyl radical scavenger [12] but has been lately found to exhibit an inhibitory effect on PARP [13]. Nicaraven protects hematopoietic stem cells against radiation injury [14] and reduces inflammation-induced cancer metastasis to the lungs in a mouse tumor model [15]. However, the direct effect of nicaraven on cancer cells has not yet been well investigated. Since the perturbation of PARylation/dePARylation has successfully achieved the selective killing of cancer cells, it is interesting to investigate the role and relevant mechanism of nicaraven on cancer cells because of the potential inhibitory effect of nicaraven on PARP [13].

In this study, we aimed to evaluate the direct effect of nicaraven on the viability of cancer cells. Using human monocyte- like lymphoma cells (U937) and human colorectal cancer cells (HCT-8) that show the comparable expression level of PARP-1 [16], we observed that nicaraven significantly induced the apoptosis and parthanatos (PAR-dependent cell death) by distinct mechanisms according to the expression levels of Bcl-2 and PARG in cancer cells.

Materials and methods

Cell culture

U937 cells and HCT-8 cells were used for the experiments. Cells were maintained in RPMI-1640 medium (Fujifilm Wako, JP) supplemented with 10% FBS (Corning, US) and 1% penicillin/streptomycin (Fujifilm Wako, JP), at 37C in a humidified atmosphere with 5% CO_2 and 95% air.

* Corresponding author at: Department of Stem Cell Biology, Atomic Bomb Disease Institute, Nagasaki University, 1-12-4 Sakamoto, Nagasaki 852-8523, Japan.
E-mail address: litaoshe@nagasaki-u.ac.jp (T.-S. Li).

https://doi.org/10.1016/j.tranon.2022.101548
Received 27 April 2022; Received in revised form 14 September 2022; Accepted 21 September 2022
Available online 4 October 2022

Cell viability assays

Cells were seeded in 96-well culture plates (5×10^3 cells/well) and cultured overnight. Cells were then treated with 0, 2, or 5 mM nicaraven (Achemblock, US). At 24 h of nicaraven treatment, a viability assay was performed using the Cell Proliferation Kit I (MTT) according to the manufacturer's protocol (Roche Diagnostics, CH). Briefly, MTT was added and incubated for 4 h. The formation of formazan was stopped by adding solubilization solution, and the absorbance was measured at 570 nm using a microplate reader (iMark™ Microplate Reader; Bio-Rad Laboratories, US).

Oxygen consumption assays

Oxygen consumption of cancer cells was measured using the Extracellular O_2 Consumption Assay Kit (Abcam, UK), according to the manufacturer's instructions. Briefly, HCT-8 cells (4×10^4 cells in 150 µl medium/well) were seeded in 96-well culture plates and incubated overnight. The culture medium was replaced with a medium containing 0 or 5 mM nicaraven. For the non-adherent U937 cells, 8×10^4 cells in 150 µl medium containing 0 or 5 mM nicaraven were seeded in each well of 96-well culture plates. Fluorescence (excitation at 380 nm; emission at 650 nm) of the dye was measured at 30 min and 24 h using a spectrophotometer (SpectraMax, Molecular devices, US).

Mitochondrial assays

To evaluate the mitochondrial membrane potential, mitochondrial mass, and mitochondrial reactive oxygen species (ROS), HCT-8 cells were treated with 0 or 5 mM nicaraven for 2 h. Then, cells were incubated with 100 nM Mitotracker Red (Thermo Fisher Scientific, US) for 45 min, 200 nM Mitotracker Green (Thermo Fisher Scientific, US) for 45 min, or 10 µM MitoSOX (Thermo Fisher Scientific, US) for 30 min, respectively; before the measurement of fluorescence intensity by spectrophotometer (SpectraMax, Molecular Devices, US).

Measurement of NAD^+ and NADH

Cells were seeded in 6 cm dishes (3.5×10^5 cells/dish), cultured overnight, and then added 0 or 5 mM nicaraven for another 24 h incubation. The concentrations of NAD^+ and NADH were determined with the NAD^+/NADH Assay Kit-WST (Dojindo, JP), following the manufacturer's protocol. Absorbance was measured at 450 nm using a microplate reader (iMark™ Microplate Reader; Bio-Rad Laboratories, US).

Flow cytometry

For the evaluation of cell apoptosis, an annexin V-FITC apoptosis staining/detection kit (Abcam, UK) was used following the manufacturer's protocol. Data acquisition and analysis were performed using the FACSVersa flow cytometer (BD Biosciences, US).

Western blotting

Cells with 0 or 5 mM nicaraven treatment were harvested, washed with PBS, and suspended in Laemmli's buffer. For the extraction of nuclear content and cytoplasmic fractions, Nuclear Extraction Kit (Abcam, UK) was used. Cell lysates were heated at 95℃ for 5 min, then loaded on SDS-PAGE gel and transferred to PVDF membrane (Bio-Rad Laboratories, US). Membranes were probed with antibodies against PARP-1, PARG, AIF, caspase-3, caspase-7, caspase-9, β-Actin, α-Tubulin (1:1000; Cell Signaling Technology, US), PAR (1:1000; Trevigen, US), Bcl-2 (1:1000; Bethyl laboratory, US), and Lamin B1 (1:1000; Abcam, UK) at 4°C overnight or 25°C for 1 h. Followed by the appropriate secondary antibodies for 1 h at 25°C, the expression was visualized using an ECL detection kit (SuperSignal West Femto, ThermoFisher Scientific, US). The blots were detected using ImageQuant LAS 4000 Mini biomolecular imager (Cytiva, US) and analyzed by ImageJ 2.1.0 software (National Institutes of Health, US).

RNA interference

Human AIF mRNA was inhibited using RNAi Duplex Oligos from TriFECTa RNAi Kit (Integrated DNA Technologies, US), following the manufacturer's instructions. Final concentrations of 0.1 nM and 1.0 nM siRNAs in Lipofectamine RNAiMAX (Invitrogen, US) were used for transfection to HCT-8 cells and U937 cells, respectively.

Immunofluorescence staining

Immunofluorescence staining was performed to detect the expression of AIF. Briefly, cells were fixed with 4% formalin (Fujifilm Wako, JP) for 10 min and permeabilized. After blocking, cells were incubated with primary antibody against AIF (1:400, Cell Signaling Technology, US) at 4℃ overnight, washed by PBST, and followed by Alexa Fluorescent 546-conjugated secondary antibody (1:1000, Thermo Fisher Scientific, US) for 1 h at 25℃ in the dark. The nuclei were labeled with DAPI. Positive staining was detected under a fluorescent microscope (Fluoview FV10i, Olympus, JP).

Molecular docking

To identify potential binding sites of nicaraven to PARP-1, PARG, and Bcl-2, we performed an automated molecular-docking procedure using the web-based SwissDock program [17,18]. The docking was performed using the 'Accurate' parameter at default parameters, with no region of interest defined (blind docking). The three-dimensional structure of PARP-1 (ID: 7kk6), PARG (ID: 6hmm), and Bcl-2 (ID: 1G5m) used as receptors were obtained from the Protein Data Bank (https://www.rcsb.org/). The structures of nicaraven, olaparib, nariparib, veliparib, acetylcysteine, aspirin, PDD00017273 Hcl, JA2131, COH34, ventoclax, and navitoclax were downloaded from the PubChem website (https://pubchem.ncbi.nlm.nih.gov/) or Zinc 15 website (https://zinc.docking.org/). Molecular graphics and analyses were performed with UCSF Chimera (National Institutes of Health, US). The lowest energy was selected as a potential binding structure.

Statistical analyses

Results are presented as mean ± SD from independent experiments with duplicates or triplicates. Statistical analysis was performed by unpaired *t*-test or paired *t*-test for comparisons between two groups, and by ANOVA for multiple comparisons using GraphPad Prism 8.0 software. Significance was determined at $p < 0.05$.

Results

Nicaraven significantly decreases the viability and metabolic activity in both U937 and HCT-8 cells

MTT assays showed that nicaraven significantly reduced the viability of both cell lines in a dose-dependent manner ($p<0.001$, Figs. 1A and S1). The metabolic rate was examined by measuring the oxygen consumption, which is essential for energy production [19,20], and 5 mM nicaraven significantly reduced the oxygen consumption in both cell lines ($p<0.05$, Fig. 1B). To further confirm the effect of nicaraven on metabolic activity, we also measured the mitochondrial membrane potential, mitochondrial mass, and mitochondrial ROS in HCT-8 cells. As expected, HCT-8 cells with 5 mM nicaraven treatment for 2 h decreased mitochondrial membrane potential and mitochondrial ROS levels ($p<0.05$, Fig. S2A&B), while the mitochondrial mass did not

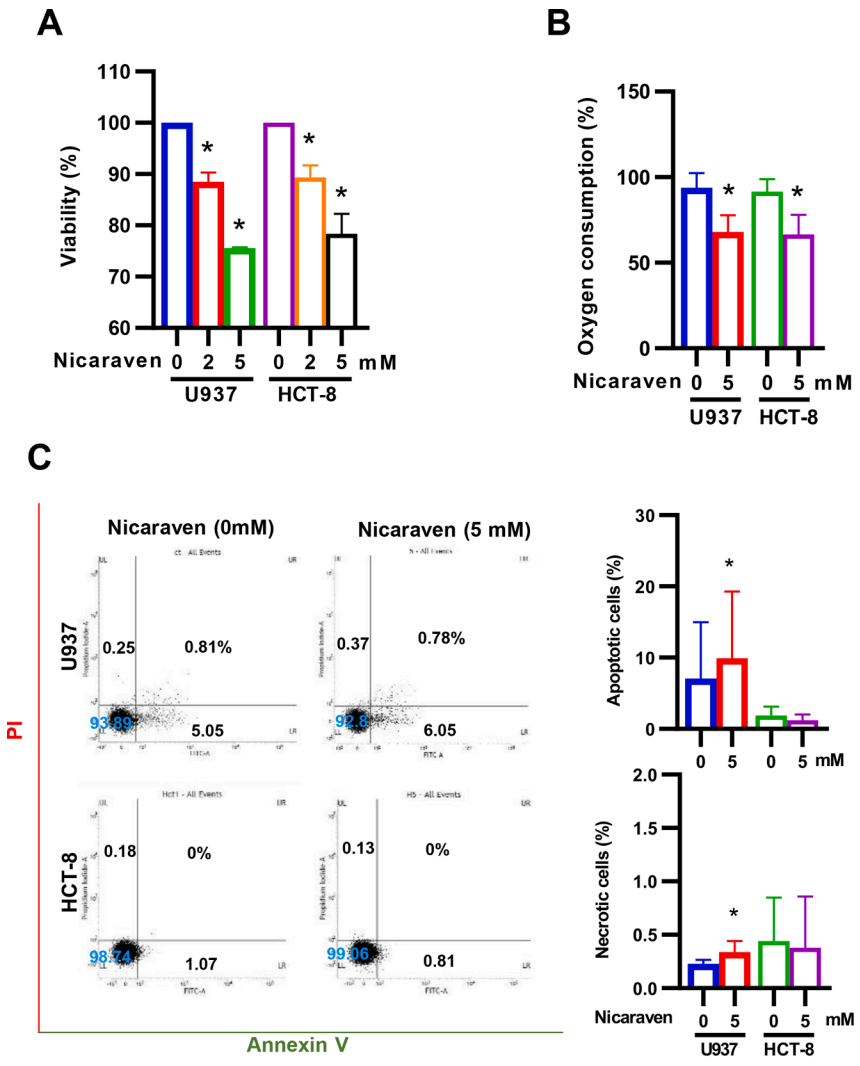

Fig. 1. The viability and the metabolic rate of cancer cells. **A**) MTT assay about the viability of cancer cells with 0, 2, 5 mM nicaraven treatment for 24 h. **B**) The relative oxygen consumption of cancer cells with 0 or 5 mM nicaraven treatment for 24 h. **C**) Flow cytometry analysis on cell death of U937 and HCT-8 cells with 0 or 5 mM nicaraven treatment for 24 h. Representative dot-graph (left) and quantitative data (right) are shown. **D**) Representative images of the morphology under phase-contrast microscopy (left panel) and the DAPI-stained nuclei under fluorescent microscopy (right panel) of U937 and HCT-8 cells with 0 or 5 mM nicaraven treatment for 24 h. Yellow arrows indicate apoptotic cells and white arrows indicate parthanatotic cells. *$p < 0.05$. Scale bars: 50 μm. Data represent the mean ± SD.

significantly change (Fig. S2C).

We also performed flow cytometry using Annexin V/PI to detect the potential cytotoxic effect of nicaraven on U937 and HCT-8 cells. Interestingly, nicaraven significantly induced apoptosis and necrosis only in U937 cells (Fig. 1C), although the MTT assay showed the inhibitory effect of nicaraven in both U937 and HCT-8 cells. To further observe directly the cytotoxic effect of nicaraven on cells under microscopy, we stained the nuclei with DAPI after nicaraven treatment for 24 h. Some morphological changes, such as cell membrane blebbing and small DNA fragmentation were detectable in U937 cells with 5 mM nicaraven treatment, suggesting cell apoptosis [21,22]. Nevertheless, we observed a morphological feature of parthanatos [22], a large DNA fragmentation

(chromatinolysis) only in HCT-8 cells after 5 mM nicaraven treatment (Fig. 1D).

PARP-1 is overexpressed in most cancer patients

We searched the genomic database for the expression levels of PARP-1, Bcl-2, and PARG in human monocyte-like lymphoma cell lines (U937 cells and HL-60 cells) and human colorectal cancer cell lines (HCT-15 cells* and HCT-116 cells, *HCT-15 cells are the same genetic origin as HCT-8 [23]). According to the Gene Atlas database (https://www.ebi.ac.uk/gxa/experiments/E-MTAB-2770/), these cell lines have a comparable level of PARP-1 expression (Fig. 2A). However, U937 cells and HL-60 cells show dominant expression of Bcl-2 compared to the colorectal cancer cell lines. In contrast, the HCT-15 cells and HCT-116 cells show higher expression of PARG compared to the U937 cells and HL-60 cells (Fig. 2A).

PARP-1 protein is highly expressed in almost all types of malignant tumors, including lymphoma and colorectal carcinoma as reported in the human protein atlas (https://www.proteinatlas.org/, Fig. 2B). Since it is reported that nicaraven has an inhibitory effect on PARP [13], we investigated the effect of nicaraven on U937 cells and HCT-8 cells because of the comparable PARP-1 expression. Albeit, the expression of Bcl-2 and PARG were differently detected between U937 cells and HCT-8 cells (Figs. 2C&D and S3).

Nicaraven upregulates caspase-7 to induce apoptosis of U937 cells with dominant Bcl-2 expression

To investigate the molecular mechanism of nicaraven in regulating cancer cell viability, we performed a Western blot analysis. Our data showed that nicaraven decreased the expression of Bcl-2 in U937 cells, while Bcl-2 was constitutively low in HCT-8 cells (Fig. 3A). Interestingly, nicaraven treatment for 60 min significantly increased caspase-7 only in U937 cells (Fig. 3B). Whereas caspase-3 was slightly enhanced in U937 cells, but decreased in HCT-8 cells (Fig. 3B). However, the expression of caspase-9 was barely affected by nicaraven treatment in both U937 cells and HCT-8 cells (Fig. S4).

We further used pan-caspase inhibitor Z-VAD to confirm whether the cytotoxic effect of nicaraven on U937 cells was mediated by caspase-dependent apoptosis. Unexpectedly, pre-treatment with Z-VAD for 3 h showed that nicaraven significantly reduced the viability of both cell lines (Fig. S5). However, the cell apoptosis (Fig. 1C) and the upregulated caspase-7 expression (Fig. 3B) in U937 cells with nicaraven treatment were effectively abrogated by Z-VAD (Fig. 3C&D). Therefore, it seems that nicaraven upregulates caspase-7 to induce apoptosis in U937 cells.

Nicaraven interferes with AIF expression to induce parthanatos of HCT-8 cells with high PARG expression

We also investigated whether PARP-1 is involved in the inhibitory

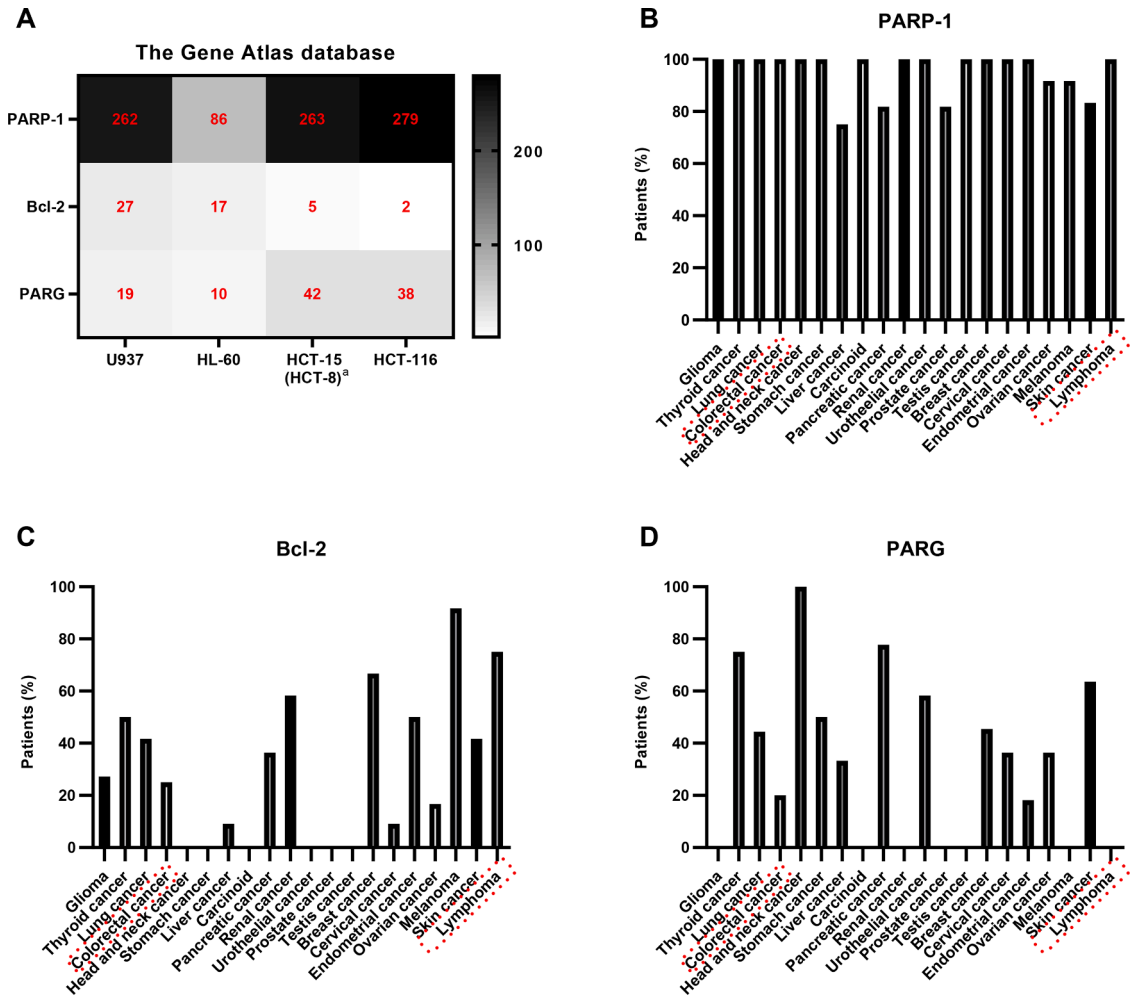

Fig. 2. The relative expression levels of PARP-1, PARG, and Bcl-2 in different cancer cell lines and malignant tumors. **A**) The relative expression levels of PARP-1, PARG, and Bcl-2 in different cancer cell lines (U937, HL-60, HCT-15, and HCT-116) based on the Gene Atlas database. Bar graphs show the positive expression rate of PARP-1 (**B**), PARG (**C**), and Bcl-2 (**D**) in different malignant tumors based on the Human Protein Atlas database. [a] HCT-8 cells are the same genetic origin as HCT-15.

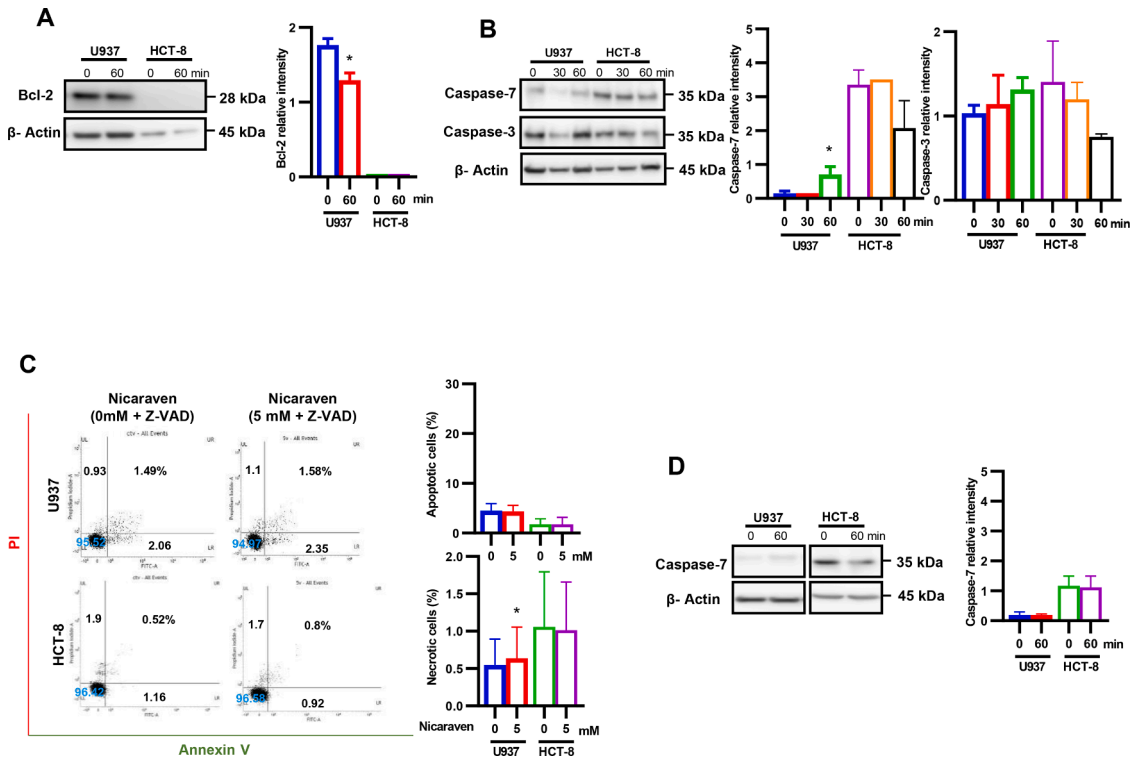

Fig. 3. Nicaraven upregulates caspase-7 to induce apoptosis of U937 cells. **A**) Western blot analysis on the expression of Bcl-2 in U937 and HCT-8 cells treated with 0 or 5 mM nicaraven for 60 min. **B**) Western blot analysis on the expression of caspase-7 and caspase-3 in U937 and HCT-8 cells treated with 0 or 5 mM nicaraven for 30 and 60 min. **C**) Flow cytometry analysis on cell death of U937 and HCT-8 cells pre-treated with 20 μM Z-VAD for 3 h, and then followed by 0 or 5 mM nicaraven treatment for 24 h. **D**) Western blot analysis on the expression of caspase-7 in U937 and HCT-8 cells pre-treated with 20 μM Z-VAD for 3 h, and then followed by 0 or 5 mM nicaraven treatment for 60 min. *p < 0.05. Data represent the mean ± SD.

effect of nicaraven on cancer cell viability. Unexpectedly, nicaraven treatment for 60 min significantly decreased the expression of PARP-1 in U937 cells but increased in HCT-8 cells (Fig. 4A). As PARP-1 regulates the formation of PAR [24], we further measured the protein level of PAR. Interestingly, nicaraven treatment for 60 min significantly induced the accumulation of high molecular weight PAR only in HCT-8 cells (p=0.012, Fig. 4A). Moreover, the expression of PARG; the main enzyme for PAR degradation [25,26], was decreased in HCT-8 cells, but conversely increased in U937 cells after nicaraven treatment (Fig. 4B).

To investigate the probable relation between PAR accumulation and parthanatos in HCT-8 cells, we analyzed the expression of AIF. Nicaraven treatment significantly increased the total and nuclear levels of AIF in HCT-8 cells (Fig. 4B&C). Immunofluorescence staining also showed that nicaraven treatment significantly increased the number of parthanatotic cells only in HCT-8 cells (Fig. 4D), indicating the probable relation between AIF expression and parthanatos.

To further confirm whether nicaraven induced parthanatos by interfering with AIF expression, we silenced AIF by siRNA (Fig. S6A&B). AIF silencing decreased the viability of HCT-8 cells with or without nicaraven treatment (Fig. S7). As expected, the nicaraven-induced parthanatos in HCT-8 cells was completely abrogated by AIF silencing (Fig. 4E). According to our data, it seems that nicaraven interferes with AIF expression to induce parthanatos of HCT-8 cells.

As NAD depletion causes parthanatos [22], we also measured NAD^+/NADH levels in both cell lines. Interestingly, nicaraven significantly decreased NAD^+/NADH levels only in HCT-8 cells (Fig. 4F).

Docking simulation on the potential binding sites of nicaraven to PARP-1, PARG, and Bcl-2

We performed a docking simulation on the potential binding sites of nicaraven (Fig. S8). The binding energies of specific inhibitors such as olaparib, nariparib, and veliparib to PARP-1 were calculated as −9.35, −9.96, and −9.74 kcal/mol, respectively. The calculated binding energy of nicaraven to PARP-1 (−8.20 kcal/mol) was higher than PARP-1 specific inhibitors, but was much lower than the free radical scavenger acetylcysteine (−6.73 kcal/mol) and the anti-inflammatory drug aspirin (−6.59 kcal/mol, Fig. 5A). Interestingly, the calculated binding energy of nicaraven to PARG (−7.92 kcal/mol) was comparable with PARG specific inhibitor of COH34 (−7.62 kcal/mol, Fig. 5B). However, nicaraven showed lower binding energy than acetylcysteine (−6.79 kcal/mol) and aspirin (−6.65 kcal/mol), indicating the higher affinity of nicaraven to PARG (Fig. 5B). Otherwise, the calculated binding energy of nicaraven to Bcl-2 was comparable with acetylcysteine (−7.28 *vs.* −7.01 kcal/mol), but was lower than aspirin (−6.74 kcal/mol, Fig. 5C). Together this data indicates that nicaraven has a higher binding affinity to PARP-1, PARG, Bcl-2 compared to acetylcysteine and aspirin.

Discussion

Nicaraven has been well documented for its effects of free radical scavenging and anti-inflammation [27], but little is known about its role in cancer cells. Using U937 lymphoma cells and HCT-8 colorectal cancer cells, we herein observed a consistent metabolic inhibition of nicaraven on cancer cells, namely the reduced oxygen consumption. In addition, we found that nicaraven decreased the viability of cancer cells in a dose-dependent manner by distinct mechanisms, according to the expression levels of PARG and Bcl-2, rather than the expression level of PARP-1.

Nicaraven has been reported to inhibit the activity of PARPs, suggesting the potential application for cancer treatment [13]. Using U937 cells and HCT-8 cells that are remarkably expressing PARP-1 at a comparable level [16], we observed that nicaraven decreased mildly but significantly the viability of both cell lines in a dose-dependent manner.

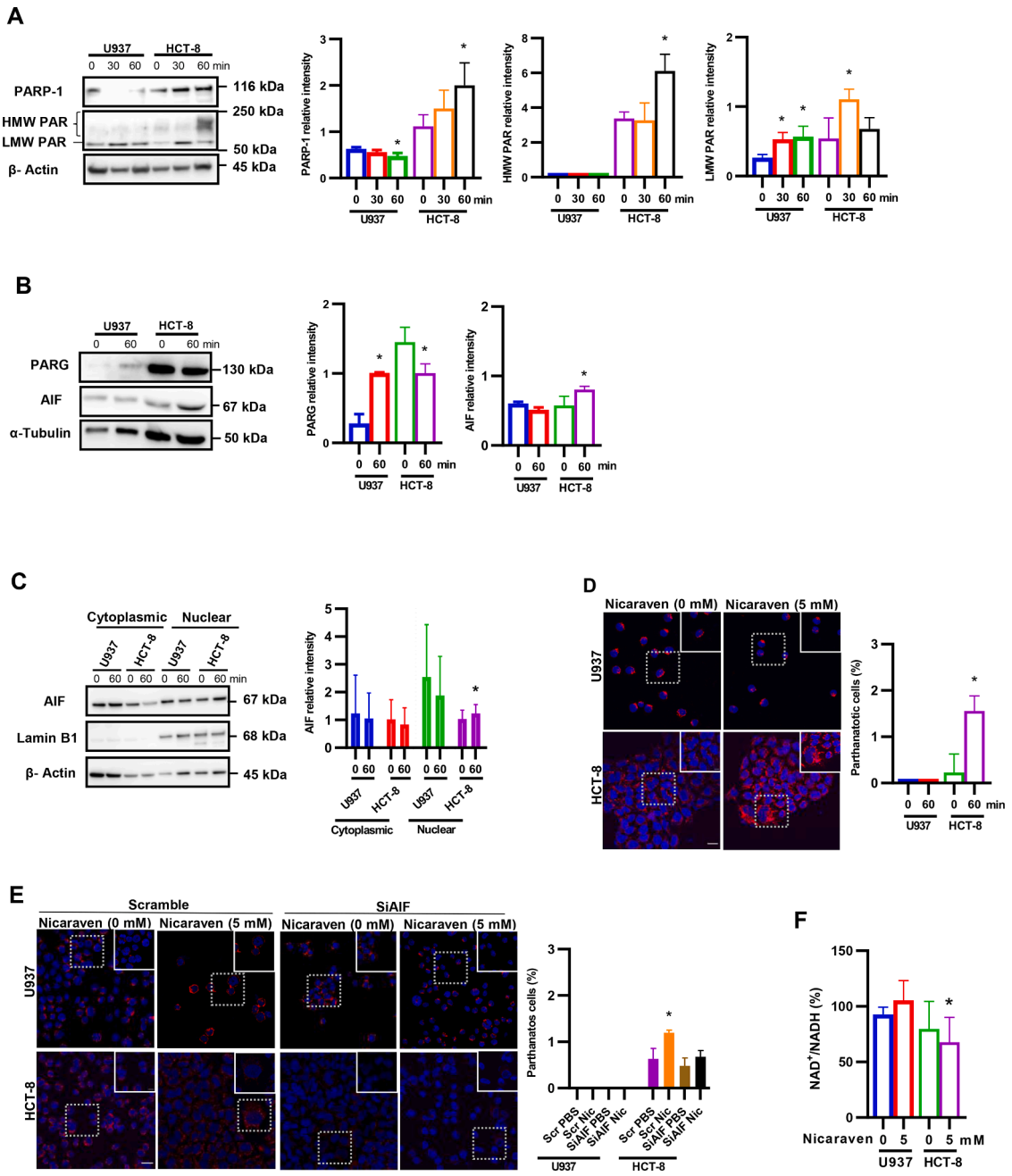

Fig. 4. Nicaraven interferes with AIF expression to induce parthanatos in HCT-8 cells. **A**) Western blot analysis on the expression of PARP-1 and PAR in U937 and HCT-8 cells treated with 0 or 5 mM nicaraven for 30 and 60 min. **B**) Western blot analysis on the expressions of PARG and AIF in U937 and HCT-8 cells treated with 0 or 5 mM nicaraven for 60 min. **C**) Western blot analysis on the cytoplasmic and nuclear levels of AIF in U937 and HCT-8 cells treated with 0 or 5 mM nicaraven for 60 min. **D**) Representative images of immunofluorescence staining for AIF in U937 and HCT-8 cells treated with 0 or 5 mM nicaraven for 60 min. Scale bars: 50 μm (or 25 μm of inset). The right bar graph represents the percentage of parthanatotic cells. **E**) Representative images of immunofluorescence staining for AIF in U937 and HCT-8 cells. Cells with or without AIF silencing were treated with 0 or 5 mM nicaraven for 60 min. Scale bars: 50 μm (or 25 μm of inset). The right bar graph represents the percentage of parthanatotic cells after treatment. **F**) The percentage of NAD^+/NADH in U937 and HCT-8 cells treated with 0 or 5 mM nicaraven for 24 h. Scr; scrambled RNA. SiAIF; small interference RNA targeting AIF. *$p < 0.05$. Data represent the mean ± SD.

Surprisingly, the change of PARP-1 expression in both cell lines with nicaraven treatment displayed opposite trends, increasing in HCT-8 cells but decreasing in U937 cells. Therefore, the effect of nicaraven on the viability of cancer cells is not closely associated with PARP-1 inhibition.

To search for the potential molecular mechanism beyond PARP-1 inhibition, we investigated whether nicaraven could induce the change in cell metabolism. In agreement with a report about the inhibition of nicaraven on mitochondrial respiration [28], our in vitro experimental data showed a slight decrease in oxygen consumption in cancer cells with nicaraven treatment. Considering that the mild change in cell metabolism may not be enough to decrease the viability of cancer cells, we further examined cell apoptosis. As expected, nicaraven promoted the apoptosis of U937 cells, which was evidenced by the small DNA fragmentation and increased annexin V-positive cell fraction. However, nicaraven did not change the annexin V-positive cell fraction in HCT-8 cells, suggesting that other mechanisms were involved in the inhibition of the cell viability in HCT-8 cells. According to the database and our experimental data, U937 cells highly express Bcl-2, a molecule

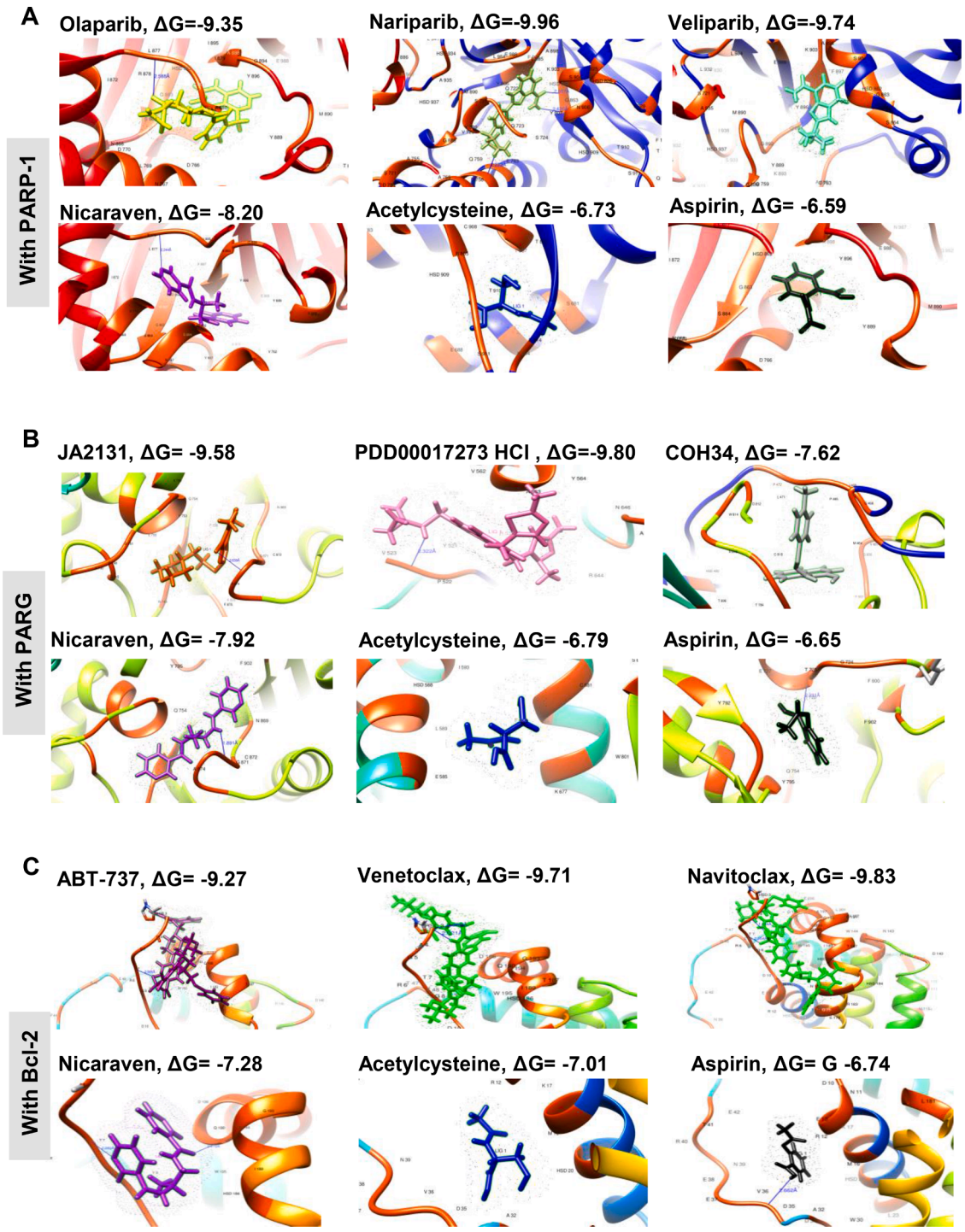

Fig. 5. Docking simulation on the potential binding sites of nicaraven to PARP-1, PARG, and Bcl-2. **A**) Binding structures of PARP-1 with the PARP-1 specific inhibitors (Olparib, Nariparib, Veliparib), nicaraven, acetylcysteine, and aspirin. **B**) Binding structures of PARG with the PARG-specific inhibitors (JA2131, PDD00017273 HCL, COH34), nicaraven, acetylcysteine, and aspirin. **C**) Binding structures of Bcl-2 with the Bcl-2 specific inhibitors (ABT-737, Venetoclax, Navitoclax), nicaraven, acetylcysteine, and aspirin. The calculated binding energies are also given.

well known to regulate cell apoptosis [29]. On one hand, we found that nicaraven induces caspase-7 to promote apoptosis in these U937 cells with dominant Bcl-2 expression. On the other hand, information from the database indicates a remarkable level of PARG expression in HCT-8 cells, which was also confirmed by our experiment. We have further demonstrated that nicaraven induces the expression and nuclear translocation of AIF, which thereby contributes to PAR-dependent parthanatos in these HCT-8 cells with high PARG expression. It was also reported that apoptosis and parthanatos could represent alternate outcomes of a similarly programmed cell death program [30,31]. It is also reported that Bcl-2 blocks the AIF parthanatos death signal [29]. Therefore, nicaraven seems to induce programmed cancer cell death through distinct mechanisms, according to the expression levels of Bcl-2 and PARG (Fig. 6).

A molecular docking simulation was performed to know the potential direct interaction of nicaraven with PARP-1, PARG, and Bcl-2. Surprisingly, nicaraven showed a high binding affinity to PARG similar to COH34, a promising PARG inhibitor [11]. Nicaraven also

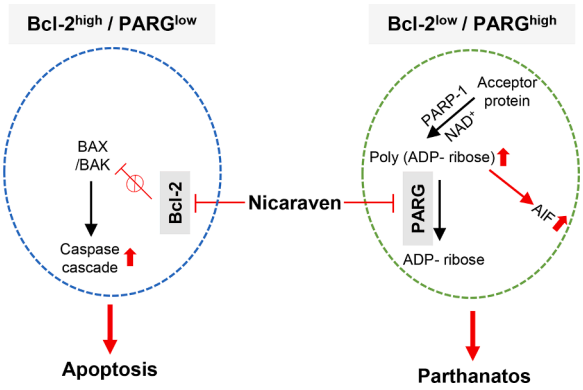

Fig. 6. Schematic diagram about the possible molecular mechanism involved in the cytotoxic effect of nicaraven on cancer cells. The left panel indicates the proposed model about how nicaraven leads to apoptotic cell death in high Bcl-2 expressing cancer cells. The right panel indicates the proposed model about how nicaraven leads to parthanatotic cell death in high PARG-expressing cancer cells.

showed remarkable binding affinity to PARP-1 and Bcl-2. Our *in vitro* experimental data are strongly supported by the results from *in silico* molecular docking simulation analysis. It is reported that anti-inflammatory drugs such as aspirin and antioxidant drugs such as acetylcysteine can be used in the prevention and neoadjuvant therapy of cancers [32–36]. Nicaraven is originally developed as a free radical scavenger [12] but recently has been reported about its anti-inflammatory property [25]. Compared to aspirin and acetylcysteine, nicaraven has a higher binding affinity to PARP-1, PARG, and Bcl-2. According to our data, nicaraven may potentiate the cytotoxic effects of chemotherapeutic agents against cancer cells.

This study has several limitations. First, the cytotoxic effect of nicaraven on cancer cells is relatively small (about 25% inhibition), which is not high enough to be declared an anti-cancer drug for chemotherapy. Second, in our *in silico* molecular docking model, the calculated binding affinities of nicaraven to PARP-1, PARG, and Bcl-2 are not the defined active sites. Therefore, the pharmacological effects of nicaraven directly targeting PARP-1, PARG, and Bcl-2 need to be confirmed by additional *in vitro* and *in vivo* experiments.

In conclusion, we have demonstrated that nicaraven presents a direct cytotoxic effect on cancer cells through distinct mechanisms according to the expression levels of Bcl-2 and PARG. Data from this study not only provide a novel insight into the molecular mechanism of nicaraven against cancer cells but also support the use of nicaraven as a promising adjuvant therapeutic drug for cancer patients.

Author contributions

LA and TL conceptualized and designed the study. LA performed the experiments, acquired the data, and drafted the manuscript. LA and TL analyzed and interpreted the data. TL, SG, and TK were consulted in the experimental method. KJ and TL gave final approval for the manuscript to be published. TL supervised the study , wrote and reviewed the final manuscript. All authors read and approved the manuscript.

Data availability statement

All data are included in the paper and/or the Supplementary material.

Declaration of Competing Interest

The authors declare that they have no known competing financial interests or personal relationships that could have appeared to influence the work reported in this paper.

Acknowledgments

This study was mainly supported by Japan Agency for Medical Research and Development under Grant Number JP20lm0203081.

Supplementary materials

Supplementary material associated with this article can be found, in the online version, at doi:10.1016/j.tranon.2022.101548.

References

[1] M. Rose, J.T. Burgess, K. O'Byrne, D.J. Richard, E. Bolderson, PARP inhibitors: clinical relevance, mechanisms of action and tumor resistance, Front. Cell Dev. Biol. 8 (2020), 564601. https://www.frontiersin.org/article/10.3389/fcell.2020.564601.

[2] M. Uhlen, C. Zhang, S. Lee, E. Sjöstedt, L. Fagerberg, G. Bidkhori, R. Benfeitas, M. Arif, Z. Liu, F. Edfors, K. Sanli, K. von Feilitzen, P. Oksvold, E. Lundberg, S. Hober, P. Nilsson, J. Mattsson, J.M. Schwenk, H. Brunnström, B. Glimelius, T. Sjöblom, P.-H. Edqvist, D. Djureinovic, P. Micke, C. Lindskog, A. Mardinoglu, F. Ponten, A pathology atlas of the human cancer transcriptome, Science 357 (2017) aan2507, https://doi.org/10.1126/science.aan2507.

[3] M. Mashimo, J. Kato, J. Moss, ADP-ribosyl-acceptor hydrolase 3 regulates poly (ADP-ribose) degradation and cell death during oxidative stress, Proc. Natl. Acad. Sci. U. S. A. 110 (2013) 18964–18969, https://doi.org/10.1073/pnas.1312783110.

[4] C. Soldani, A.I. Scovassi, Poly (ADP-ribose) polymerase-1 cleavage during apoptosis : an update Cell death mechanisms : necrosis and apoptosis, Apoptosis 7 (2002) 321–328, https://doi.org/10.1023/a:1016119328968.

[5] Y. Zhou, L. Liu, S. Tao, Y. Yao, Y. Wang, Q. Wei, A. Shao, Y. Deng, Parthanatos and its associated components: promising therapeutic targets for cancer, Pharmacol. Res. 163 (2021), 105299, https://doi.org/10.1016/j.phrs.2020.105299.

[6] E. Matta, A. Kiribayeva, B. Khassenov, B.T. Matkarimov, A.A. Ishchenko, Insight into DNA substrate specificity of PARP1-catalysed DNA poly(ADP-ribosyl)ation, Sci. Rep. 10 (2020) 1–11, https://doi.org/10.1038/s41598-020-60631-0.

[7] J. Murai, S.N. Huang, B.B. Das, A. Renaud, Y. Zhang, J.H. Doroshow, J. Ji, S. Takeda, Y. Pommier, Trapping of PARP1 and PARP2 by clinical PARP inhibitors, Cancer Res. 72 (2012) 5588–5599, https://doi.org/10.1158/0008-5472.CAN-12-2753.

[8] J.C. Brenner, F.Y. Feng, S. Han, S. Patel, V. Siddharth, L.M. Bou-maroun, M. Liu, R. Lonigro, J.R. Prensner, S.A. Tomlins, A.M. Chinnaiyan, A. Arbor, PARP-1 inhibition as a targeted strategy to treat Ewing ' s sarcoma, Cancer Res. 72 (2012) 1608–1613, https://doi.org/10.1158/0008-5472.CAN-11-3648.

[9] A. Addioui, A. Belounis, S. Cournoyer, C. Nyalendo, R.-M. Brito, M. Beaunoyer, P. Teira, H. Sartelet, Preclinical study of a PARP inhibitor in neuroblastoma, J. Clin. Oncol. 30 (2012) 9570, https://doi.org/10.1200/jco.2012.30.15_suppl.9570.

[10] A.E.O. Fisher, H. Hochegger, S. Takeda, K.W. Caldecott, Poly(ADP-ribose) polymerase 1 accelerates single-strand break repair in concert with poly(ADP-ribose) glycohydrolase, Mol. Cell. Biol. 27 (2007) 5597–5605, https://doi.org/10.1128/MCB.02248-06.

[11] M.A. Kassab, L.L. Yu, X. Yu, Targeting dePARylation for cancer therapy, Cell Biosci 10 (2020) 1–9, https://doi.org/10.1186/s13578-020-0375-y.

[12] M.S. Alam, K. Ku, M. Hashimoto, S. Nosaka, Y. Saitoh, M. Yamauchi, S. Masumura, K. Nakayama, K. Tamura, Hydroxyl radical scavenging effect of nicaraven in myocardial and coronary endothelial preservation and reperfusion injury, Cardiovasc. Res. 33 (1997) 686–692, https://doi.org/10.1016/S0008-6363(96)00268-4.

[13] M. Watanabe, N. Akiyama, H. Sekine, M. Mori, Y. Manome, Inhibition of poly (ADP-ribose) polymerase as a protective effect of nicaraven in ionizing radiation- and ara-C-induced cell death, Anticancer Res. 26 (2006) 3421–3427, https://doi.org/10.1016/0250-7005/anticanres.2006.

[14] H. Ali, O. Galal, Y. Urata, S. Goto, C. Guo, L. Luo, E. Abdelrahim, Y. Ono, E. Mostafa, T. Li, Potential benefits of nicaraven to protect against radiation-induced injury in hematopoietic stem /progenitor cells with relative low dose exposures, Biochem. Biophys. Res. Commun. 452 (2014) 548–553, https://doi.org/10.1016/j.bbrc.2014.08.112.

[15] C. Yan, L. Luo, Y. Urata, S. Goto, T.S. Li, Nicaraven reduces cancer metastasis to irradiated lungs by decreasing CCL8 and macrophage recruitment, Cancer Lett. 418 (2018) 204–210, https://doi.org/10.1016/j.canlet.2018.01.037.

[16] J. Barretina, G. Caponigro, N. Stransky, K. Venkatesan, A.A. Margolin, S. Kim, C. J. Wilson, J. Lehár, G.V Kryukov, D. Sonkin, A. Reddy, M. Liu, L. Murray, M. F. Berger, J.E. Monahan, P. Morais, J. Meltzer, A. Korejwa, J. Jané-Valbuena, F. A. Mapa, J. Thibault, E. Bric-Furlong, P. Raman, A. Shipway, I.H. Engels, J. Cheng, G.K. Yu, J. Yu, P. Aspesi, M. de Silva, K. Jagtap, M.D. Jones, L. Wang, C. Hatton, E. Palescandolo, S. Gupta, S. Mahan, C. Sougnez, R.C. Onofrio, T. Liefeld, L. MacConaill, W. Winckler, M. Reich, N. Li, J.P. Mesirov, S.B. Gabriel, G. Getz, K. Ardlie, V. Chan, V.E. Myer, B.L. Weber, J. Porter, M. Warmuth, P. Finan, J. L. Harris, M. Meyerson, T.R. Golub, M.P. Morrissey, W.R. Sellers, R. Schlegel, L. A. Garraway, The Cancer Cell Line Encyclopedia enables predictive modelling of

anticancer drug sensitivity, Nature 483 (2012) 603–607, https://doi.org/10.1038/nature11003.
[17] A. Grosdidier, V. Zoete, O. Michielin, SwissDock, a protein-small molecule docking web service based on EADock DSS, Nucl. Acid. Res. 39 (2011) W270–W277, https://doi.org/10.1093/nar/gkr366.
[18] A. Grosdidier, V. Zoete, O. Michielin, Fast docking using the CHARMM force field with EADock DSS, J. Comput. Chem. 32 (2011) 2149–2159, https://doi.org/10.1002/jcc.21797.
[19] H.-M. Kang, J.-S. Lee, Y.H. Lee, M.-S. Kim, H.G. Park, C.-B. Jeong, J.-S. Lee, Body size-dependent interspecific tolerance to cadmium and their molecular responses in the marine rotifer Brachionus spp, Aquat. Toxicol. 206 (2019) 195–202, https://doi.org/10.1016/j.aquatox.2018.10.020.
[20] D.H. Pistole, J.D. Peles, K. Taylor, Influence of metal concentrations, percent salinity, and length of exposure on the metabolic rate of fathead minnows (*Pimephales promelas*), Comp. Biochem. Physiol. Part C Toxicol. Pharmacol. 148 (2008) 48–52, https://doi.org/10.1016/j.cbpc.2008.03.004.
[21] L. Galluzzi, J.M.Bravo-San Pedro, I. Vitale, S.A. Aaronson, J.M. Abrams, D. Adam, E.S. Alnemri, L. Altucci, D. Andrews, M. Annicchiarico-Petruzzelli, E.H. Baehrecke, N.G. Bazan, M.J. Bertrand, K. Bianchi, M.V. Blagosklonny, K. Blomgren, C. Borner, D.E. Bredesen, C. Brenner, M. Campanella, E. Candi, F. Cecconi, F.K. Chan, N. S. Chandel, E.H. Cheng, J.E. Chipuk, J.A. Cidlowski, A. Ciechanover, T.M. Dawson, V.L. Dawson, V. De Laurenzi, R. De Maria, K.M. Debatin, N.Di Daniele, V.M. Dixit, B.D. Dynlacht, W.S. El-Deiry, G.M. Fimia, R.A. Flavell, S. Fulda, C. Garrido, M. L. Gougeon, D.R. Green, H. Gronemeyer, G. Hajnoczky, J.M. Hardwick, M. O. Hengartner, H. Ichijo, B. Joseph, P.J. Jost, T. Kaufmann, O. Kepp, D.J. Klionsky, R.A. Knight, S. Kumar, J.J. Lemasters, B. Levine, A. Linkermann, S.A. Lipton, R. A. Lockshin, C. López-Otín, E. Lugli, F. Madeo, W. Malorni, J.C. Marine, S. J. Martin, J.C. Martinou, J.P. Medema, P. Meier, S. Melino, N. Mizushima, U. Moll, C. Muñoz-Pinedo, G. Nuñez, A. Oberst, T. Panaretakis, J.M. Penninger, M.E. Peter, M. Piacentini, P. Pinton, J.H. Prehn, H. Puthalakath, G.A. Rabinovich, K. S. Ravichandran, R. Rizzuto, C.M. Rodrigues, D.C. Rubinsztein, T. Rudel, Y. Shi, H. U. Simon, B.R. Stockwell, G. Szabadkai, S.W. Tait, H.L. Tang, N. Tavernarakis, Y. Tsujimoto, T.Vanden Berghe, P. Vandenabeele, A. Villunger, E.F. Wagner, H. Walczak, E. White, W.G. Wood, J. Yuan, Z. Zakeri, B. Zhivotovsky, G. Melino, G. Kroemer, Essential versus accessory aspects of cell death: Recommendations of the NCCD 2015, Cell Death Differ. 22 (2015) 58–73, https://doi.org/10.1038/cdd.2014.137.
[22] D. Tang, R. Kang, T. Vanden Berghe, P. Vandenabeele, G. Kroemer, The molecular machinery of regulated cell death, Cell Res 29 (2019) 347–364, https://doi.org/10.1038/s41422-019-0164-5.
[23] S.J. Vermeulen, T.R. Chen, F. Speleman, F. Nollet, F.M. Van Roy, M.M. Mareel, Did the four human cancer cell lines DLD-1, HCT-15, HCT-8, and HRT-18 originate from one and the same patient? Cancer Genet. Cytogenet. 107 (1998) 76–79, https://doi.org/10.1016/s0165-4608(98)00081-8.
[24] S.A. Andrabi, N.S. Kim, S. Yu, H. Wang, D.W. Koh, M. Sasaki, J.A. Klaus, T. Otsuka, Z. Zhang, R.C. Koehler, P.D. Hurn, G.G. Poirier, V.L. Dawson, T.M. Dawson, Poly (ADP-ribose) (PAR) polymer is a death signal, PNAS 10 (2006) 18308–18313, https://doi.org/10.1073/pnas.0606526103.
[25] Y. Sasaki, H. Fujimori, M. Hozumi, T. Onodera, T. Nozaki, Y. Murakami, K. Ashizawa, K. Inoue, F. Koizumi, M. Masutani, Dysfunction of poly (ADP-Ribose) glycohydrolase induces a synthetic lethal effect in dual specificity phosphatase 22-deficient lung cancer cells, Cancer Res 79 (2019) 3851–3861, https://doi.org/10.1158/0008-5472.CAN-18-1037.
[26] H. Nagashima, C.K. Lee, K. Tateishi, F. Higuchi, M. Subramanian, S. Rafferty, L. Melamed, J.J. Miller, H. Wakimoto, D.P. Cahill, Poly(ADP-ribose) glycohydrolase inhibition sequesters NAD+ to potentiate the metabolic lethality of alkylating chemotherapy in IDH-mutant tumor cells, Cancer Discov. 10 (2020) 1673–1689, https://doi.org/10.1158/2159-8290.CD-20-0226.
[27] H. Lin, X. Wu, Y. Yang, Z. Wang, W. Huang, L.-F. Wang, Q.-W. Liu, X.-H. Guan, K.-Y. Deng, T.-S. Li, Y. Qian, H.-B. Xin, Nicaraven inhibits TNFα-induced endothelial activation and inflammation through suppressing NF-κB signaling pathway, Can. J. Physiol. Pharmacol. (2020), https://doi.org/10.1139/cjpp-2020-0558.
[28] B. Zingarelli, G.S. Scott, P. Hake, A.L. Salzman, C. Szabo, Effects of nicaraven on nitric oxide-related pathways and in shock and inflammation, Shock 13 (2000) 126–134, https://doi.org/10.1097/00024382-200013020-00006.
[29] Y. Tsujimoto, Role of Bcl-2 family proteins in apoptosis: apoptosomes or mitochondria? Genes to Cell. 3 (1998) 697–707, https://doi.org/10.1046/j.1365-2443.1998.00223.x.
[30] C. Artus, H. Boujrad, A. Bouharrour, M.-N. Brunelle, S. Hoos, V.J. Yuste, P. Lenormand, J.-C. Rousselle, A. Namane, P. England, H.K. Lorenzo, S.A. Susin, AIF promotes chromatinolysis and caspase-independent programmed necrosis by interacting with histone H2AX, EMBO J. 29 (2010) 1585–1599, https://doi.org/10.1038/emboj.2010.43.
[31] R.S. Moubarak, V.J. Yuste, C. Artus, A. Bouharrour, P.A. Greer, J. Menissier-de Murcia, S.A. Susin, Sequential activation of poly(ADP-ribose) polymerase 1, calpains, and Bax is essential in apoptosis-inducing factor-mediated programmed necrosis, Mol. Cell. Biol. 27 (2007) 4844–4862, https://doi.org/10.1128/MCB.02141-06.
[32] G. Maity, A. De, A. Das, S. Banerjee, S. Sarkar, S.K. Banerjee, Aspirin blocks growth of breast tumor cells and tumor-initiating cells and induces reprogramming factors of mesenchymal to epithelial transition, Lab. Investig. 95 (2015) 702–717, https://doi.org/10.1038/labinvest.2015.49.
[33] D.A. Drew, Y. Cao, A.T. Chan, Aspirin and colorectal cancer: the promise of precision chemoprevention, Nat. Rev. Cancer. 16 (2016) 173–186, https://doi.org/10.1038/nrc.2016.4.
[34] J. Hybiak, I. Broniarek, G. Kiryczyński, L.D. Los, J. Rosik, F. Machaj, H. Sławiński, K. Jankowska, E. Urasińska, Aspirin and its pleiotropic application, Eur. J. Pharmacol. 866 (2020), 172762, https://doi.org/10.1016/j.ejphar.2019.172762.
[35] D. Monti, F. Sotgia, D. Whitaker-menezes, R. Birbe, A. Berger, M. Lazar, P. Cotzia, R. Draganova-tacheva, Z. Lin, M. Domingo-vidal, M.P. Lisanti, U. Martinez-outschoorn, Pilot study demonstrating metabolic and anti-proliferative effects of in vivo anti-oxidant sup-plementation with N-Acetylcysteine in breast cancer, Semin. Oncol. 44 (2018) 226–232, https://doi.org/10.1053/j.seminoncol.2017.10.001.Pilot.
[36] Y. Kwon, Possible beneficial effects of N-acetylcysteine for treatment of triple-negative breast cancer, Antioxidants 10 (2021) 169, https://doi.org/10.3390/antiox10020169.